RESEARCH ARTICLE | SEPTEMBER 08 2023

Enhancing the control strategy of fault ride through capability for grid connected wind farm using VSC_HVDC

Dalya H. Al-Mamoori ✉; Zinah S. Hasan; Ali Assim Al-Obaidi; M. H. Mussa

AIP Conf. Proc. 2804, 050006 (2023)
https://doi.org/10.1063/5.0154771

Enhancing the Control Strategy of Fault Ride through Capability for Grid Connected Wind Farm Using VSC_HVDC

Dalya H. Al-Mamoori[1, a)], Zinah S. Hasan[2], Ali Assim Al-Obaidi[3], and M. H. Mussa[4, b)]

[1] *Technical College Al-Musaib, Al-Furat Al- Awsat Technical University, Babil, Iraq*
[2] *Faculty of Engineering, Universiti Teknologi Malaysia (UTM), Johor Bahru, Johor, Malaysia*
[3] *Technical Institute of Babylon, Al-Furat Al- Awsat Technical University, Babil, Iraq*
[4] *College of Engineering, University of Warith Al-Anbiyaa, Karbala, Iraq*

[a)] Corresponding author: daliahamza784@atu.edu.iq
[b)] dr.mhmussa@uowa.edu.iq

Abstract. This paper is aimed to design a power system which contains 20 arrangements of 2MW 11kV wind turbines a 40 MW offshore wind farm is simulated trendy PSCAD/EMTDC. The power is formerly transported through HVDC lines and linked to the grid. The fault ride through (FRT)for the wind farm is organized through VSC-HVDC.By review two stages 6-pulse Disconnected (IGBT) Tyristors at the generator and grid side of the system two voltage source converter stations are simulated in PSCAD/EMTDC software. The control arrangement is joint in the middle of situations in statute to develop the (FRT) and voltage instruction for the wind farm. The wind turbine governor controls the pitch angle using power output and the generator speed. The pitch angle will change respectively in order to reduce the changes in the generator's rotor speed. By decreasing the changes in rotor speed, wind turbine is able to generate more constant power with less effect on the power transmission and the control system can be used to reduce the effect of fault in wind farm side to fulfill the E.On requirements for increase the fault ride-through capability of the wind farm and that the duration of the fault plays a vital part in decision making for wind farms disconnection. This control system can be used for offshore wind farms linked to the grid where the wind farm is able to continue its operation without disconnection during the fault times.

Keywords. Fault ride through; HVDC system, Wind farm; VSC-HVDC transmission, PSCAD/EMTDC software

INTRODUCTION

The cause of global warming is the permanent fiery of vestige fuels and the gases emitted from them. This takes controlled administrations to pay care to utilize of green energy as an alternative of fossil petroleum. Wind machinery is a practical alternate to creating electric, and several countries in the world specifically Europe have observed growth and development in the use of wind farms to generate electricity. However, several issues the systems through HVDC are still exist owing to control complexity high price of convertor stations and semiconductor failures. The first commercial HVDC transmission line was built between Gotland and mainland Sweden in 1954. Although the advantages of HVDC was clear in comparison with HVAC systems high prices of two rectifier stations and high number of failure in semiconductors have been the main challenge to decide using HVDC system instead of HVAC [1]. As power generation increased from hundred MWs to thousand MWs which were needed to be transmitted for longer distances, the power losses in HVAC configuration in one hand and cost of three conductors instead of two in HVDC configuration on the other hand make this system more preferred than HVAC [2]. The break even distance for these two configurations can be determined by referring to the amount of power and transmission line distance [3]. The longer the distance, the more losses in HVAC system due to AC lines reactive characteristics. There is no such

The Fourth Scientific Conference for Electrical Engineering Techniques Research (EETR2022)
AIP Conf. Proc. 2804, 050006-1–050006-9; https://doi.org/10.1063/5.0154771
Published by AIP Publishing. 978-0-7354-4637-3/$30.00

loss in DC cables because of zero frequency in DC links [4-9]. Moreover, the independency of frequency makes the HVDC system a great choice for off shore wind farms despite changes in the wind speed and turbine rotation speed [10-21].

Sang et al.[22] Suggested a disconcertion approximation-built nonlinear adaptive control (NAC) designed for a (VSC-HVDC) system and indicated that this strategy could improve dynamic behavior in the event of process with a variation of compact voltage stages. Khani [23] offered a new control strategy established on liberating calculated reactive power by (STATCOM) which avoiding voltage breakdown is realized throughout the fault. Tzelepis et al. [24] suggests a DC voltage control strategy for fault managing and proved that this strategy could reflect as an operational method of continuing the DC overvoltage inside safety boundaries via decreasing the linked to wind farm power production.

The grid code used in this paper is EOn grid code [25]. This control system can be used for offshore wind farms linked to the grid where the wind farm is able to continue its operation without disconnection during the fault times. This ability makes the wind farms more reliable especially when wind farms become the main source of power in the network.

E.ON CODE REQUIREMENT

According to EOn grid code, the changes in the voltage is needed to be in acceptable area, else the wind farm will have to be separated from the grid [26-31] . The EOn grid code requirement for duration of voltage sag is presented in Fig. 1. The Low voltage ride through desires of EOn grid code [10], the wind turbines requisite stay linked when connecting point voltage residues intimate the shadow region up to boundary line 1. A short disconnection is allowable, when the connecting point voltage is between lines 1 and 2. The tenacity of this paper is to control the voltage to stay in the Area 1.

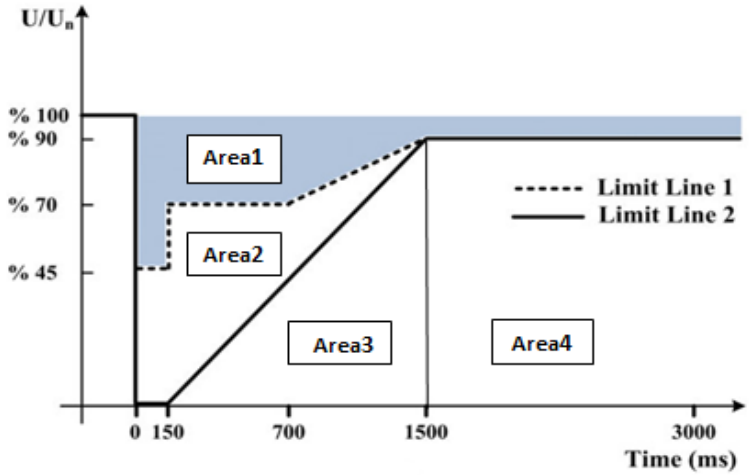

FIGURE 1. EOn grid code requirement for duration of voltage sag.

Modelling of the power system

In this paper, Fig. 3 shows the power system which contains 20 arrangements of 2MW 11kV wind turbines a 40 MW wind farm is simulated trendy PSCAD/EMTDC. The power is formerly transported through HVDC lines and linked to the grid. The fault ride through (FRT) for the wind farm is organized through VSC-HVDC. By review two stages 6-pulse Disconnected (IGBT) Tyristors at the generator and grid side of the system two (VSC) stations are simulated. Control arrangement is joint in the middle of situations in statute to develop the (FRT) and voltage instruction for the wind farm. Where, ph1 is the anticipated period angle and m1 is the anticipated voltage amount for generator lateral converter, ph2 is the period angle and m2 is the voltage amount for grid lateral converter and P,Q are active and reactive power between 2 nodes in alternating circuit system , U1 and U2. Θ is the phase-angle change and is the line reactance amid the two nodes [38].The output power of the turbine can be calculated via (1) equation, Chavero et al [32].

$$P(v) = \frac{1}{2}.\rho.A.v^3.C_p\ (\lambda, \beta) \quad (1)$$

Where the equation parameters are:

(P) is the output power.

(A) is wind turbine area.

(ρ) is the air density (v) is the wind.

(C_P) is coefficient factor should be less than 0.59 and can be calculated as follows:

$$C_P=0.22(\frac{116}{\beta} - 0.40 - 5)e^{-\frac{12.5}{\beta}} \quad (2)$$

Where the equation parameters are:

β is pitch angle of the wind turbine blades.

λ ,θ is the angle in degree of the tip speed ratio .

These parameters determined as follows:

$$\beta = \frac{1}{\frac{1}{\lambda + 0.08\theta} - \frac{0.035}{\theta^3 + 1}} \quad (3)$$

$$\lambda = R\frac{w}{v} \quad (4)$$

The AC three phase voltages in generator side are converted to DC. Voltage in DC side can be calculated as follows[33]:

$$U_d = \frac{3\sqrt{2}}{\pi}.V_u.cos\ cos\ \alpha \quad (5)$$

Where the equation parameters are:

(U_d) is the DC voltage and α is the firing angle.

(V_u) is the line voltage of AC side.

It is clearly shown that when α is equal to 90 degrees the DC voltage is equal to zero and when α is equal to zero the voltage in DC side is maximum. The firing angle in converters is determined by changing the firing time of IGBTs. In generator side, the firing time for IGBT valves are fixed permitted to transmit the extreme power. The active and reactive power in DC side can be intended by using the following equations [20]:

$$P = -\frac{3}{2}V_s\ \frac{L_m}{L_s}\ i_{rq} \quad (6)$$

$$Q = \frac{3}{2}\{\frac{V_s^2}{w_s L_S} - \frac{V_s\ \ L_m\ i_{rd}}{L_s}\} \quad (7)$$

Where the equation parameters are:

(P) is active power

(Q) is reactive power

(V_s) is the phase voltage of the stator side of the generator.

(i_{rq}) and (i_{rd}) are the quadratic and direct current of the stator.

So as to control the voltage sag, it is essential to control the reactive power generated by wind farm. From equations (6) and (7),[34]. It can be realized that the active and reactive power can be organized respectively via regulatory i_{rq} and i_{rd}. In inverter side, the converter station is connected to the grid and controls the voltage in the DC link. Figure 2 shows the power output of 2MW wind turbine for several wind speed and different air densities.

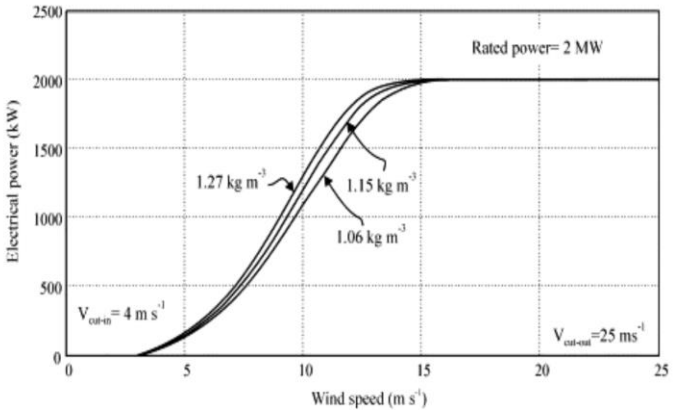

FIGURE 2. Power output of 2MW wind turbine for different wind speed and different air densities [4].

It can be seen in Fig. 2 that the output is constant from 15m/s to 25 m/s. It shows that the pitch is adjusted in a way that turbine rotates in its rated value.

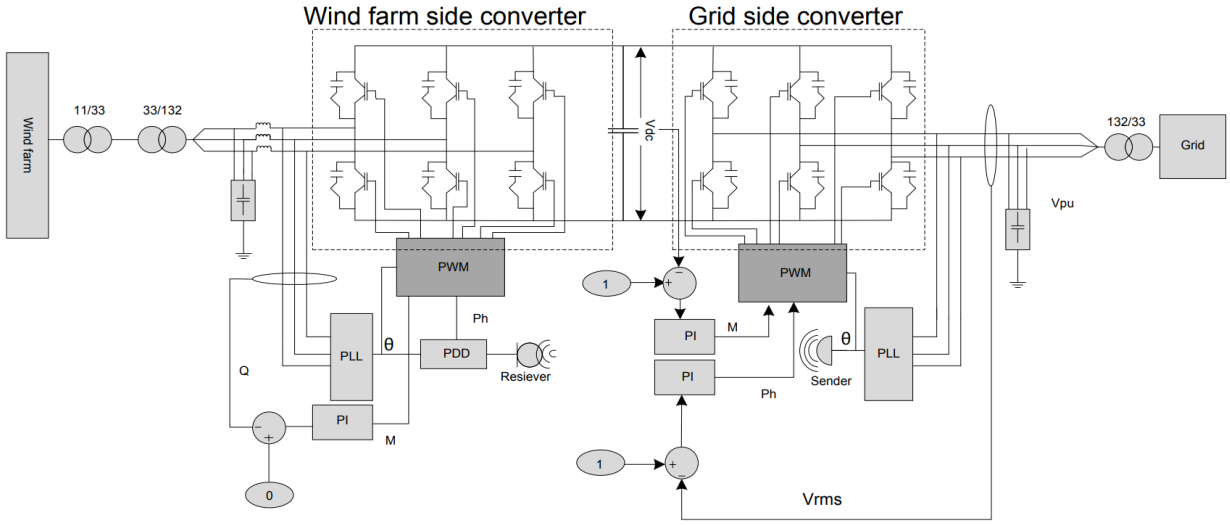

FIGURE 3. The system simulated in PSCAD/EMTDC.

Voltage control strategy

Active and reactive power generation by wind farm is needed to be controlled during the fault times. In the rectifier side, the power is controlled and wind farm inject reactive power to the connection point to increase the voltage and decrease the voltage sag in the wind farm side. This control scheme is based on equations (2) and (3). By controlling the i_{rq} and i_{rd}, wind farm is able to generate reactive power without the effect on real power generation. Figures 4 and 5 are shown the control strategy on rectifier side. Simple PI controller is used due to its simplicity in design [20,35-37].

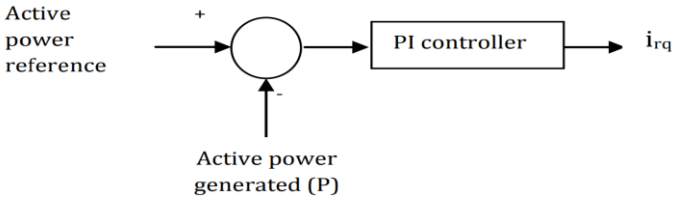

FIGURE 4. i_{rq} control system.

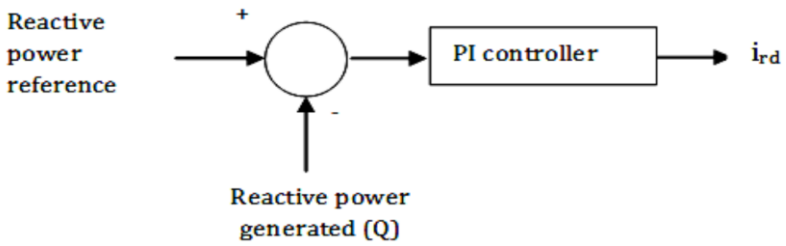

FIGURE 5. i_{rd} control system.

Active power is controlled by controlling i_{rq} and reactive power can be organized by controlling i_{rd}. The reference currents generated by PI controller then are fed to d_q to abc converter component to generate the three phase reference currents. Moreover, using a pulse wide modulation (PWM) the firing pulses for IGBTs will be generated. On the grid crosswise, voltage is needed to be controlled to decrease the voltage sag in DC link. Control strategy used in grid side of the transmission system. V_{rms} is compared with the reference V_{rms} and V_{dc} is compared with $V_{dc-reference}$. Using simple PI controller, reference voltage for PWM is generated. Three phase reference voltages are then generated using d_q to abc converter. Rotating angle for qd to ABC converter is generated through PLL component.

SIMULATION RESULTS

The wind turbine governor controls the pitch angle using power output and the generator speed. Figure 6 shows the generator speed and pitch angle during modifications in wind velocity. When the wind changes for 10 seconds, pitch angle then will increase to reduce the rotor speed and maintain the rotation of the shaft in the acceptable speed area. In Fig. 6, during the time that wind speed is changing the pitch angle will change respectively in order to reduce the changes in the generator's rotor speed. By decreasing the changes in rotor speed, wind turbine is able to generate more constant power with less effect on the power transmission. The voltage in grid side and wind farm side are shown in Figs. 7 to 11.

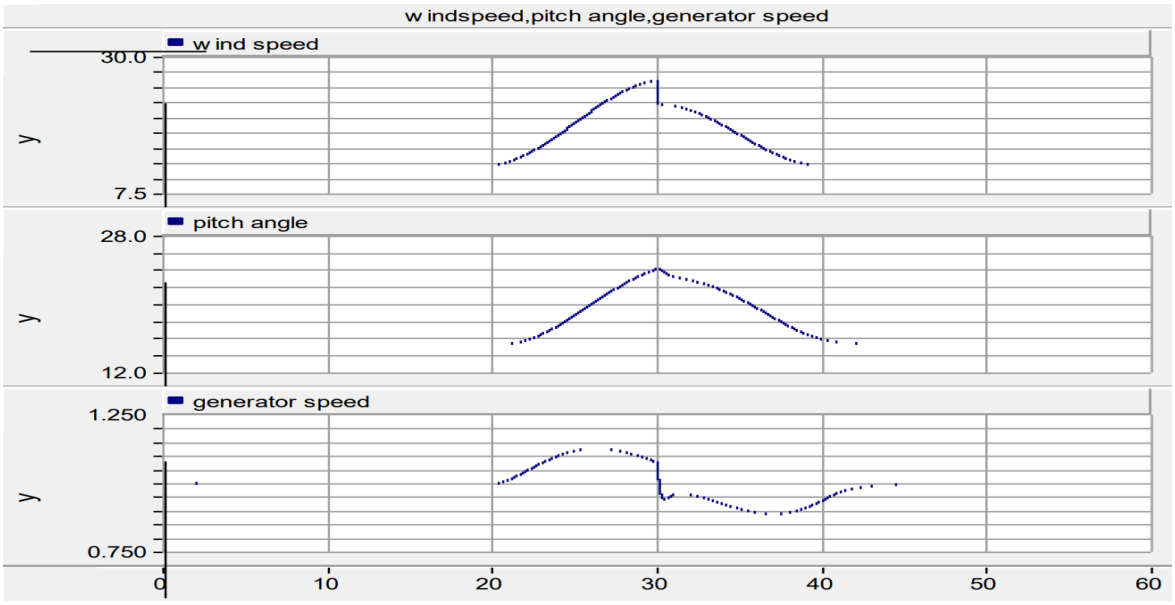

FIGURE 6. The generator speed and pitch angle during changes in wind velocity.

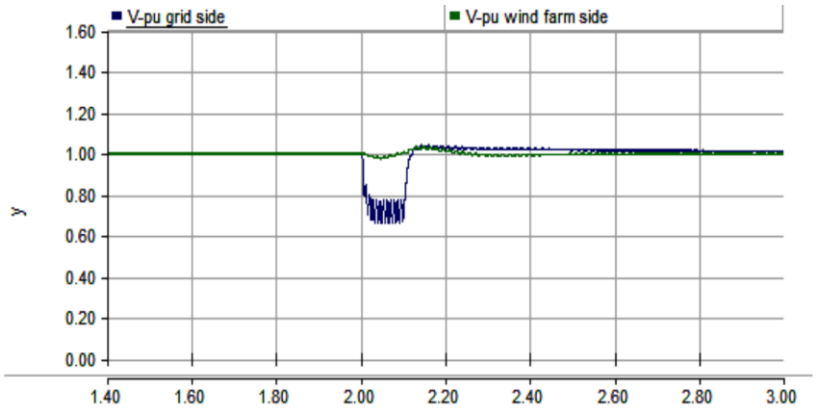

FIGURE 7. Voltage sag in grid side and wind farm side for fault (a).

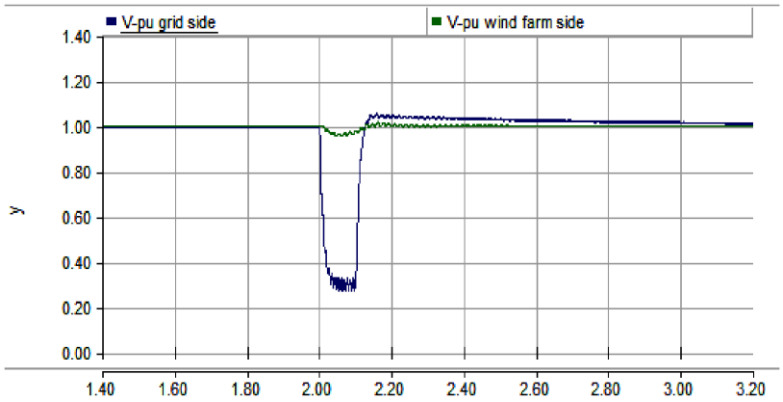

FIGURE 8. Voltage sag in grid side and wind farm side for fault (b).

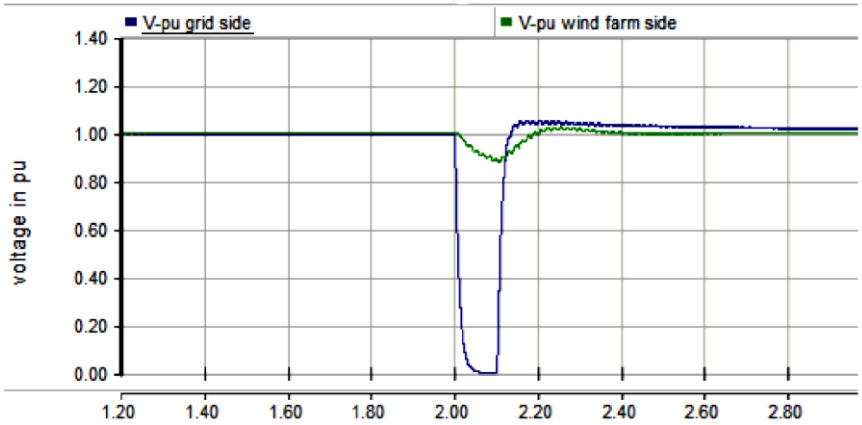

FIGURE 9. Voltage sags in grid side and wind farm side for fault (c).

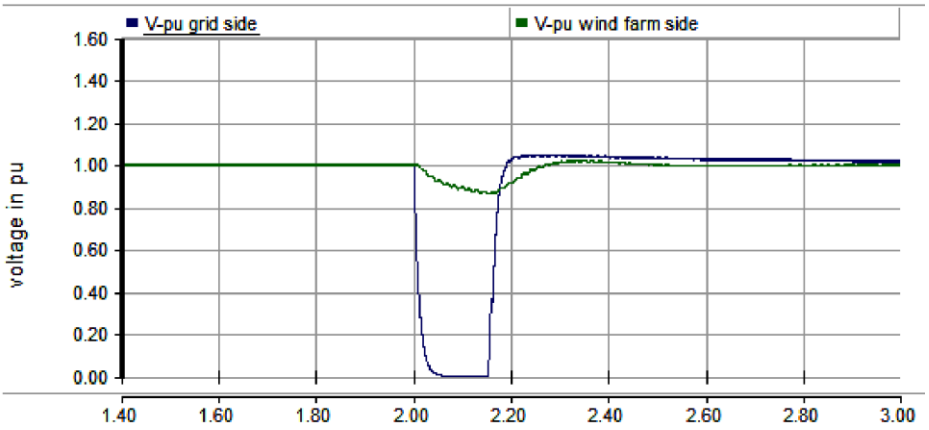

FIGURE 10. Voltage sag in grid side and wind farm side for fault (d).

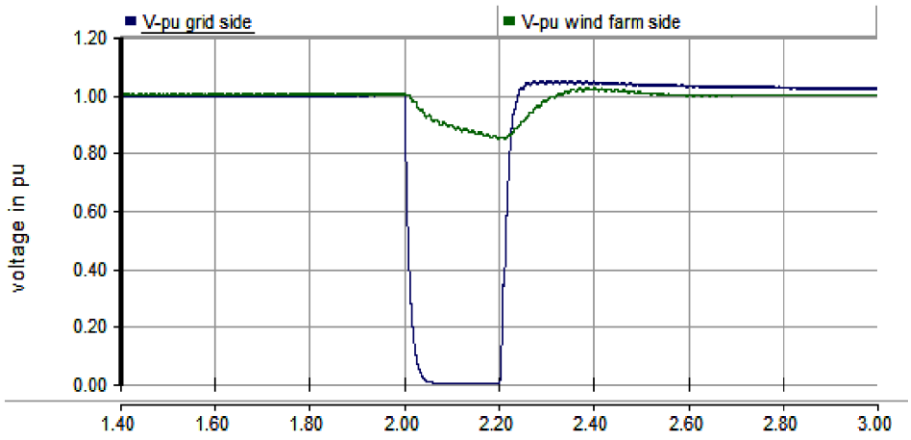

FIGURE 11. Voltage sag in grid side and wind farm side for fault (e).

CONCLUSION

The fault ride through capability of 40 MW offshore wind farm remained examined. The proposed control method of the offshore wind farm using VSC-HVDC is able to ride through grid fault and realizes the EOn grid code requests. The simulation results as well expression that the interval of grid fault plays a role in defining the ride through capability of the wind. The result also shows that the duration of the fault plays a vital part in decision making for wind farm disconnection.

REFERENCES

1. Asongu SA, Agboola MO, Alola AA, et al. The criticality of growth, urbanization, electricity and fossil fuel consumption to environment sustainability in Africa. Science of the Total Environment. 2020;712:136376.
2. Bizhani H, Noroozian R, Muyeen S, et al. Wind farm grid integration architecture using unified expandable power converter. IEEE Transactions on Power Electronics. 2018;34(4):3407-3417.
3. Zakzouk NE, Abdelsalam AK, Helal AA, et al. PV single-phase grid-connected converter: dc-link voltage sensorless prospective. IEEE Journal of Emerging and Selected Topics in Power Electronics. 2016;5(1):526-546.
4. Franck CM. HVDC circuit breakers: A review identifying future research needs. IEEE transactions on power delivery. 2011;26(2):998-1007.

5. Paez JD, Frey D, Maneiro J, et al. Overview of DC–DC converters dedicated to HVdc grids. IEEE Transactions on Power Delivery. 2018;34(1):119-128.
6. Al-Obaidi AA, Salman AJ, Yousif AR, et al. Characterization the effects of nanofluids and heating on flow in a baffled vertical channel. International Journal of Mechanical and Materials Engineering. 2019;14(1):1-15.
7. Mussa MH, Mutalib AA, Hamid R, et al. Assessment of damage to an underground box tunnel by a surface explosion. Tunnelling and Underground Space Technology. 2017;66:64-76.
8. Mussa MH, Radzi NAM, Hamid R, et al. Fire Resistance of High-Volume Fly Ash RC Slab Inclusion with Nano-Silica. Materials. 2021;14(12):3311.
9. Mussa MH, Abdulhadi AM, Abbood IS, et al. Late age dynamic strength of high-volume fly ash concrete with nano-silica and polypropylene fibres. Crystals. 2020;10(4):243.
10. Takahashi R, Tamura J, Futami M-O, et al. A new control method for wind energy conversion system using a doubly-fed synchronous generator. IEEJ Transactions on Power and Energy. 2006;126(2):225-235.
11. Zakzouk NE, Elsaharty MA, Abdelsalam AK, et al. Improved performance low-cost incremental conductance PV MPPT technique. IET Renewable Power Generation. 2016;10(4):561-574.
12. Xiang X, Zhang X, Chaffey GP, et al. An isolated resonant mode modular converter with flexible modulation and variety of configurations for MVDC application. IEEE Transactions on Power Delivery. 2017;33(1):508-519.
13. Al-Mamoori DH, Neda OM, Al-Tameemi ZH, et al., editors. Generating High Voltage DC with Cockcroft-Walton Voltage Multiplier for Testing Locally Assemble Electric Field Sensor. IOP Conference Series: Materials Science and Engineering; 2019: IOP Publishing.
14. Abedini M, Mutalib AA, Zhang C, et al. Large deflection behavior effect in reinforced concrete columns exposed to extreme dynamic loads. Frontiers of Structural and Civil Engineering. 2020;14(2):532-553.
15. Zhang G, Ali ZH, Aldlemy MS, et al. Reinforced concrete deep beam shear strength capacity modelling using an integrative bio-inspired algorithm with an artificial intelligence model. Engineering with Computers. 2020:1-14.
16. Mussa MH, Mutalib AA. Effect of geometric parameters (β and τ) on behaviour of cold formed stainless steel tubular X-joints. International Journal of Steel Structures. 2018;18(3):821-830.
17. Mussa MH, Mutalib AA, Hamid R, et al. Blast damage assessment of symmetrical box-shaped underground tunnel according to peak particle velocity (PPV) and single degree of freedom (SDOF) criteria. Symmetry. 2018;10(5):158.
18. Mutalib AA, Mussa MH, Hao H. Effect of CFRP strengthening properties with anchoring systems on PI diagrams of RC panels under blast loads. Construction and Building Materials. 2019;200:648-663.
19. Abbood IS, Mahmod M, Hanoon AN, et al. Seismic response analysis of linked twin tall buildings with structural coupling. International Journal of Civil Engineering and Technology 2018; 9(11):208-219.
20. Abedini M, Khlaghi EA, Mehrmashhadi J, et al. Evaluation of Concrete Structures Reinforced with Fiber Reinforced Polymers Bars: A Review. Journal of Asian Scientific Research. 2017;7(5):165.
21. Alhawat H, Hamid R, Bahroom S, et al. A review on large-scale fire testing of concrete tunnel lining. Journal of Engineering and Applied Sciences. 2019;14(9):2891-2897.
22. Sang Y, Yang B, Shu H, et al. Fault ride-through capability enhancement of type-4 WECS in offshore wind farm via nonlinear adaptive control of VSC-HVDC. Processes. 2019;7(8):540.
23. Khani NG. Improving fault ride through capability of induction generator-based wind farm using static compensator during asymmetrical faults. International Transactions on Electrical Energy Systems. 2021;31(11):e13103.
24. Tzelepis D, Rousis AO, Dysko A, et al. Enhanced DC voltage control strategy for fault management of a VSC-HVDC connected offshore wind farm. 2016.
25. ON E. Requirements for Off-Shore Grid Connection in the E. On Nets Network, E ON Nets GmbH, Bayreuth, Germany. 2008.
26. Al-Mamoori DH, Aljanabi MH, Neda OM, et al. Evaluation of gas fuel and biofuel usage in turbine. Indonesian Journal of Electrical Engineering and Computer Science. 2019;14(3):1097-1104.
27. Al-Tameemi ZH, Neda OM, Jumaa FA, et al., editors. Optimal Sizing and Location of DG Units for Enhancing Voltage Profile and Minimizing Real Power Losses in the Radial Power Systems Based on PSO Technique. IOP Conference Series: Materials Science and Engineering; 2019: IOP Publishing.
28. Olabi A. Renewable energy and energy storage systems. Elsevier; 2017. p. 1-6.

29. Mussa MH, Mutalib AA, Hamid R, et al. Dynamic properties of high volume fly ash nanosilica (HVFANS) concrete subjected to combined effect of high strain rate and temperature. Latin American Journal of Solids and Structures. 2018;15(1).
30. Mussa MH, Mutalib AA, Hamid R, et al., editors. Advanced dynamic response analysis of under-ground tunnel affected by blast ground distance. The 5th International Technical Conference (ITC); 2020; Malaysia.
31. Mussa MH, Mutalib AA, Hao H. Numerical formulation of PI diagrams for blast damage prediction and safety assessment of RC panels. Structural Engineering and Mechanics. 2020;75(5):607-620.
32. Chavero-Navarrete E, Trejo-Perea M, Jáuregui-Correa J-C, et al. Pitch angle optimization by intelligent adjusting the gains of a PI controller for small wind turbines in areas with drastic wind speed changes. Sustainability. 2019;11(23):6670.
33. Alejandro Franco J, Carlos Jauregui J, Toledano-Ayala M. Optimizing wind turbine efficiency by deformable structures in smart blades. Journal of Energy Resources Technology. 2015;137(5).
34. González-González A, Cortadi AJ, Galar D, et al. Condition monitoring of wind turbine pitch controller: A maintenance approach. Measurement. 2018;123:80-93.
35. Abd Mutalib A, Mussa MH, Abusal KMK. Numerical Evaluation of Concrete Filled Stainless Steel Tube for Short Columns Subjected to Axial Compression Load. Jurnal Teknologi. 2018;80(2).
36. Abedini M, Mutalib AA, Raman SN, et al. Numerical investigation on the non-linear response of reinforced concrete (RC) columns subjected to extreme dynamic loads. Journal of Asian Scientific Research. 2017;7(4):86.
37. Saadun A, Mutalib AA, Hamid R, et al. Behaviour of polypropylene fiber reinforced concrete under dynamic impact load. Journal of Engineering Science and Technology. 2016;11(5):684-693.